

Numerical studies of the spatial and temporal distributions of seismic events under different confining conditions

Qi Zhao¹, Nicola Tisato¹, Andrea Lisjak², Omid K. Mahabadi², and Giovanni Grasselli¹

¹Department of Civil Engineering, University of Toronto, Canada

²Geomechanica Inc., Canada

q.zhao@mail.utoronto.ca

Summary

The studies of the influences of confining pressure (P_c) on the damage and failure of rocks are valuable for mining activities and hydrocarbon explorations. Often, these activities need geophysical surveillance and can be monitored by studying the associated seismic energy release (i.e. induced seismicity). For example, in hydraulic fracturing operations, microseismic (MS) activities are widely used to monitor and optimize stimulations. Similarly, at the laboratory scale compression tests and the associated acoustic emissions (AE) are utilized to characterize rock failure.

In this contribution, we used the combined finite and discrete element method (FDEM) to examine the spatial and temporal distribution patterns of AE in confined compression tests conducted on the Stanstead Granite. P_c conditions ranging from 0 to 6 MPa which corresponding to the rock brittle macroscopic response are considered in this work. We studied AE that occurred before and after the yielding stress (peak point) separately. Simulations demonstrated that under the same P_c , AE were more diffused at pre-peak stage and clustered at post-peak stage, which was illustrated by the drop of the spatial fractal dimension (D-value). On the other hand, D-value remained almost constant at pre-peak stage regardless the variation of P_c , but increased with increasing P_c at the post-peak stage, indicating that the confining condition influences the transition in spatial distribution patterns between pre- and post-peak stages. Moreover, simulations showed that the drop in D-value is closely related to the increase in AE rate, and at low confinement, these variations are more pronounced and the rock tended to fail rapidly; contrarily, when P_c is relatively high, these variations are minimal and the rock remained intact.

Introduction

AE generated by fracturing processes are often utilized to investigate damage in rock volumes during laboratory tests (Lockner, 1993; Lei et al., 2004). Since small scale fracturing are found to obey similar statistics as large seismic activities, laboratory observations regarding AE are indicative for studies on crustal or regional seismic activities (Lockner, 1993). However, these laboratory experiments are destructive tests requiring much preparation and resources. Meanwhile, numerical methods simulating crack nucleation and propagation have been improved, and it is possible to use numerical simulations to gain detailed insights into seismic activities (e.g., Hazzard & Young, 2000; Lisjak et al., 2013; Zhao et al., 2014). We utilize FDEM to simulate AE in compression tests on Stanstead Granite at the laboratory scale under various confining pressure (P_c) conditions. FDEM has the ability to explicitly capture the entire loading and failure path (Mahabadi, 2012; Lisjak et al., 2013) and the associated seismic activities (Zhao et al., 2014).

Theory and/or Method

Two-dimensional (2-D) biaxial tests subjected to P_c were modelled in this study. In a FDEM model, the rock sample is discretized using an unstructured triangular finite element mesh. Elastic triangular elements represent the mineral grains composing the rock, and are connected each other by four-noded cohesive elements, which represent grain boundaries (Munjiza, 2004; Mahabadi et al., 2012). Such cohesive elements can deform elastically according to the force exerted on them and eventually break when the slip or the opening displacement is excessively large. FDEM has the ability to capture the elastic deformation of different solids, crack propagation, and corresponding particle motions (Munjiza, 2004; Mahabadi et al., 2012).

In this study, properties of the Stanstead Granite were assigned to the numerical rock sample and the spatial heterogeneity of mineral phases was stochastically generated based on a discrete Poisson distribution of the rock mineral composition (Mahabadi, 2012). Parameters assigned to the Stanstead Granite model were chosen according to (Mahabadi, 2012) and Lisjak et al. (2013). Detailed model calibration procedure and laboratory compression tests results can be found in Mahabadi (2012). AE events were recorded using the internal monitoring approach introduced and verified by Lisjak et al. (2013). Y-Geo (Mahabadi et al., 2012) and its graphical user interface Y-GUI (Mahabadi et al., 2010) were used to build and run the FDEM models.

The temporal distribution of AE is quantitatively characterized by AE rate, which is calculated by dividing the total number of events occurred in a stage over the simulated duration of this stage. On the other hand, the spatial distribution of AE is evaluated by employing the spatial fractal dimension (D-value) following the approach in Hirata (1987). In a 2-D scenario, $D=2$ implies complete randomness, whereas the smaller D , the higher degree of clustering.

Examples

A series of simulations were carried out with confining condition ranging from 0 to 6 MPa. The increasing P_c modifies the failure behaviour of rocks. Macroscopically, the unconfined rock tended to fail by lateral splitting. Once P_c was imposed, vertical fracturing was limited, and events occurred along tilted shear bands oriented approximately 20° from the vertical axis. This angle gradually increased to 30° with increasing P_c . Such observations agree with the literature (Cook, 1976; Hoek & Brown, 1980).

Regardless of P_c , AE events, at the pre-peak stage, have relatively low magnitude and they are randomly spatially distributed (e.g. Figure 1a and c). In contrast, during the post-peak stage, AE events are more clustered at low P_c than at high P_c (e.g. Figure 1b vs 1d). These observations are mathematically captured by the variation of D-value. Pre-peak D-value is relatively stable at 1.56. However, at post-peak stage, D-value increases from 1.25 to 1.54 with P_c increases from 0 to 6 MPa. To further investigate the variation of D-value with increasing P_c , we consider also the change of the relative AE rate.

AE rates are calculated for pre- and post-peak stages according to their simulated durations (Figure 2a). Simulations indicate that during the pre-peak stage, AE rates are very low, and they decrease gradually with increasing P_c . On the other hand, during the post-peak stage, AE rates, in low confined rocks, are significantly higher than higher confined ones. The influence of P_c on AE rate becomes much more significant during the post-peak stage. AE rates at low P_c (0 - 2 MPa) are exponentially higher than those recorder for higher P_c (Figure 2a). We interpret that generally, at pre-peak stage, samples experience steady-state deformation independently of the applied confining stress; at post-peak stage, low confined samples go through unstable rapid and large deformations, while highly confined samples are able to mobilize friction at all fracture interface, resulting in less dynamic failure motions.

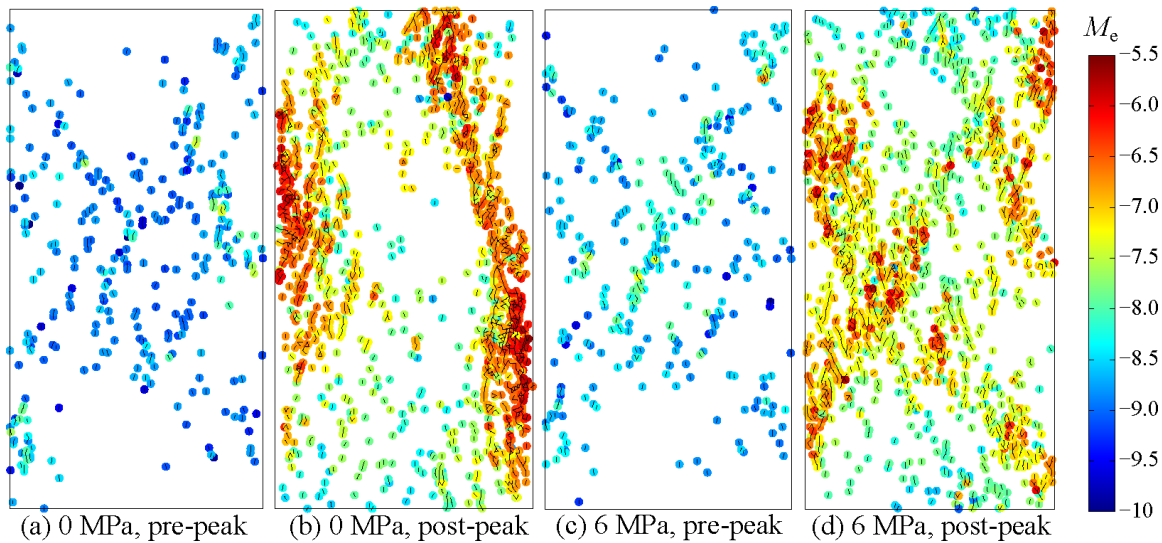


Figure 1. AE location and magnitude (M_e), taking the unconfined and 6 MPa confined simulations as examples.

Under the same confining condition, the drop of D-value, which occurs during the transit between pre- and the post-peak, is caused by the coalescence of microfractures and the spatial localization of the fracturing process. At low P_c , the D-value drops significantly, which is related to the highly concentrated intensive damage along fault planes; meanwhile at relatively high P_c , the D-value drops very little which indicates that the deformation styles before and after peak are similar.

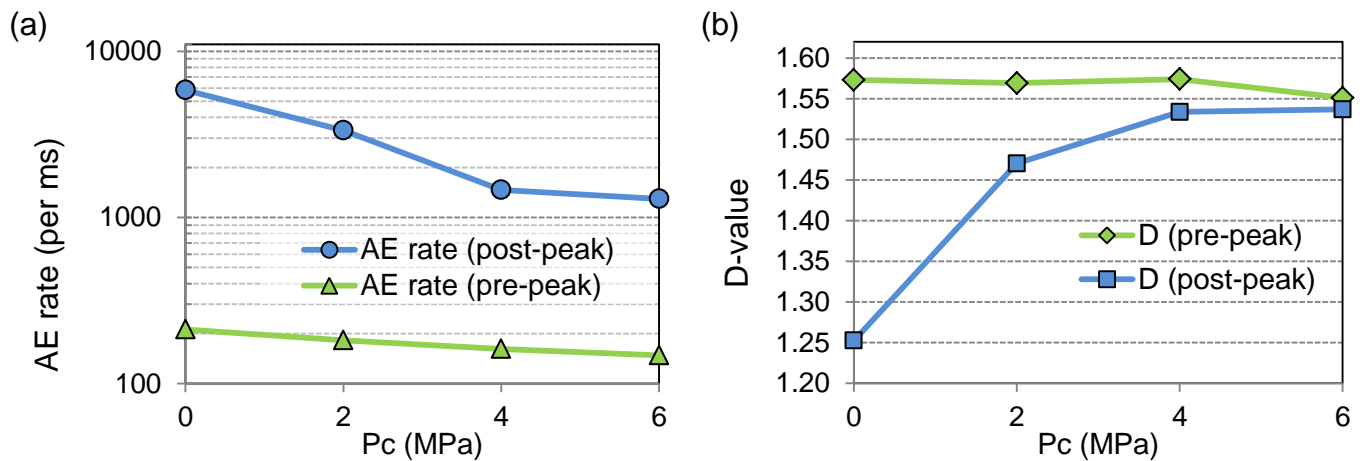


Figure 2. (a) AE rate for pre- and post-peak stages of simulations; and (b) D-values calculated for pre- and post-peak stages of simulations.

The difference between the D-values measured during the pre- and the post-peak decreases. This variation indicates that at high P_c , microfractures in rocks tend to be more homogeneous in terms of spatial distribution. This observation was also reported in the literature (Johnson, 1992). Considering the through-going faults in the low confined samples (e.g. Figure 1a), the dramatic drop of D-value may be considered a precursor to the failure of the rock (Hirata et al., 1987), and the dramatically increased AE rates in these samples agree with such interpretation.

Conclusions

We investigated the brittle deformation and failure of rocks using the FDEM approach, and we quantitatively assessed spatial and temporal distributions of AE. Simulations demonstrated that (1) P_c promotes diffused damage and decreases the AE rate; (2) damage localization (drop in D-value) which is accompanied by the increase in AE rate; and (3) the influence of P_c on AE activities is more significant during the post-peak rather than the pre-peak. These observations correspond well with the literature showing the potential of FDEM in simulating induced seismicity. Further development, such as three dimensional (3-D) simulations, will provide even more powerful tools to carry out realistic and complex simulations.

Acknowledgements

This work has been supported by the Natural Sciences and Engineering Research Council of Canada through Discovery Grant 341275 (G. Grasselli).

References

- Cook, N. G. W., 1976. Seismicity Associated with Mining. *Engineering Geology*, 10(2-4), 99-122.
- Hazzard, J. F. & Young, R. P., 2000. Simulating acoustic emissions in bonded-particle models of rock. *International Journal of Rock Mechanics and Mining Sciences*, 37(5), 867-872.
- Hirata, T., 1987. Omori's Power Law aftershock sequences of microfracturing in rock fracture experiment. *Journal of Geophysical Research: Solid Earth*, 92(B7), 6215-6221.
- Hirata, T., Satoh, T. & Ito, K., 1987. Fractal Structure of Spatial-Distribution of Microfracturing in Rock. *Geophysical Journal of the Royal Astronomical Society*, 90(2), 369-374.
- Hoek, E. & Brown, E. T. 1980. *Underground excavations in rock*.
- Johnson, E., 1992. Process Region Changes for Rapidly Propagating Cracks. *International Journal of Fracture*, 55(1), 47-63.
- Lei, X., Masuda, K., Nishizawa, O., Jouniaux, L., Liu, L., Ma, W., et al., 2004. Detailed analysis of acoustic emission activity during catastrophic fracture of faults in rock. *Journal of Structural Geology*, 26(2), 247-258.
- Lisjak, A., Liu, Q., Zhao, Q., Mahabadi, O. K. & Grasselli, G., 2013. Numerical simulation of acoustic emission in brittle rocks by two-dimensional finite-discrete element analysis. *Geophysical Journal International*, 195(1), 423-443.
- Lockner, D., 1993. The Role of Acoustic-Emission in the Study of Rock Fracture. *International Journal of Rock Mechanics and Mining Sciences & Geomechanics Abstracts*, 30(7), 883-899.
- Mahabadi, O. K. 2012. *Investigating the influence of micro-scale heterogeneity and microstructure on the failure and mechanical behaviour of geomaterials*. (Ph.D.), University of Toronto.
- Mahabadi, O. K., Grasselli, G. & Munjiza, A., 2010. Y-GUI: A graphical user interface and pre-processor for the combined finite-discrete element code, Y2D, incorporating material heterogeneity. *Computers & Geosciences*, 36(2), 241-252.
- Mahabadi, O. K., Lisjak, A., Munjiza, A. & Grasselli, G., 2012. Y - Geo: A New Combined Finite - Discrete Element Numerical Code for Geomechanical Applications. *International Journal of Geomechanics*, 1, 153.
- Munjiza, A. 2004. *The Combined Finite-Discrete Element Method*. John Wiley & Sons, Ltd.
- Zhao, Q., Lisjak, A., Mahabadi, O., Liu, Q. & Grasselli, G., 2014. Numerical simulation of hydraulic fracturing and associated microseismicity using finite-discrete element method. *Journal of Rock Mechanics and Geotechnical Engineering*, 6(6), 574-581.